15th World Congress on Computational Mechanics (WCCM-XV)
8th Asian Pacific Congress on Computational Mechanics (APCOM-VIII)
Virtual Congress: 31 July – 5 August 2022
S. Koshizuka (Ed.)

TOPOLOGY OPTIMIZATION OF ACOUSTIC-POROELASTIC-ELASTIC STRUCTURES FOR SOUND ATTENUATION

RODRIGO L. PEREIRA[1], LIDY M. ANAYA-JAMES[1] AND RENATO PAVANELLO[1]

[1] Department of Computational Mechanics, School of Mechanical Engineering, University of Campinas, Rua Mendeleyev 200, 13083-860, Campinas, Brazil
pereira@fem.unicamp.br, lidy@fem.unicamp.br, pava@fem.unicamp.br

Key words: Topology optimization, BESO method, Multiphysics, Poroelastic materials, Vibroacoustics

Abstract. *Structures for sound attenuation have been explored in many scenarios, ranging from civil construction to automotive and aerospace industries. However, the proper multiphysics interactions of acoustic-poroelastic-elastic structures are still challenging, especially when topology optimization techniques are involved. This work entails a new topology optimization methodology based on the Bi-directional Evolutionary Structural Optimization (BESO) approach to design bidimensional structures for sound attenuation enhancements. The full modeling of poroelastic bodies is done by the mixed **u**/p technique. At the same time, the elastic and acoustic (air) materials are obtained by the degeneration of the latter, leading to the well-known elasto-dynamic and Helmholtz formulations, respectively. Such procedure is done in by the combination of the Finite Element Method (FEM) with the Unified Multi-phase (UMP) modeling approach, which in turn contributes to the development of material interpolation schemes suited for the application. In this scenario, the topology optimization problem is established as the maximization of the time-averaged dissipative power, composed by the summation of its structural, viscous and thermal dissipative components. The numerical examples show the effectiveness of the proposed methodology since it provides well-defined topologies with generally enhanced dissipative performances.*

1 INTRODUCTION

This paper presents a methodology to maximize the time-averaged dissipated power. It is considered a multiphysics system composed of acoustic, elastic and poroelastic elements. The Bi-directional Evolutionary Structural Optimization (BESO) method is chosen as the optimizer, since it provides clearly defined boundaries throughout the entire optimization process. The first ones to use a similar optimization methodology were Xie and Steven [1], with the proposition of the Evolutionary Structural Optimization (ESO) method. In this case, the aim was to gradually remove inefficient material from the structure, while enhancing some physical properties of the system. In 1999, Yang et al. [2] modified the ESO technique by allowing not only material removal, but also addition to the design domain. After a series of modifications that included sensitivity filters [3] and material interpolation schemes [4], Huang and Xie [5] proposed the new BESO approach, being extensively used ever since.

As this work also deals with acoustic, elastic and poroelastic materials, careful attention has to be paid to the boundary tracking problem in a context of topology optimizations. For example, when acoustic elements change to elastic or poroelastic, the coupling between the boundaries has to be properly imposed. However, such procedure is not straightforward, in a way that a few solutions have been proposed

to overcome this issue. Yamamoto et al. [6] considered three distinct poroelastic materials inside the design domain, modifying specific variables in order to fully simulate acoustic, elastic and poroelastic structures within the same region. The success of this approach was due to the fact that the materials were all derived from Biot's equation, therefore being naturally coupled with each other. In the same year, the Unified Multiphase (UMP) technique was proposed by Lee [7, 8], which used these same Biot's equations, in the $\mathbf{u}/p$ form, as a foundation to describe the aforementioned medias. The main difference between both approaches concerns the amount of different porous materials needed in the methodology. While Yamamoto's [6] approach used three different poroelastic medias, Lee's [7, 8] considered only one.

Finally, this work also proposes a new material interpolation scheme for systematic material changes along the iterative procedure. According to Pereira et al. [9], the interpolations are generally polynomial functions of the design variables, first used in density-based approaches [4]. Besides, penalty variables are often used as degrees of freedom of the polynomial function. Although the BESO method does not need material interpolations, it has been shown that such a procedure contributes to the avoidance of singularities, as well as to the reduction of computational costs involved in multiphysics problems [10, 11].

2 FINITE ELEMENT FORMULATION FOR POROELASTIC MEDIA: THE MIXED U/P

As of 1956, Biot [12, 13] proposed expressions that were able to microscopically describe the behavior of the wave in poroelastic media, being mainly based on the displacements of the elastic ($\ddot{\mathbf{u}}$) and fluid components ($\ddot{\mathbf{U}}$), that is,

$$\nabla \cdot \underline{\boldsymbol{\sigma}}^s = \rho_{11}\ddot{\mathbf{u}} + \rho_{12}\ddot{\mathbf{U}} + \tilde{b}(\dot{\mathbf{u}} - \dot{\mathbf{U}}), \tag{1}$$

$$\nabla \cdot \underline{\boldsymbol{\sigma}}^f = \rho_{22}\ddot{\mathbf{U}} + \rho_{12}\ddot{\mathbf{u}} - \tilde{b}(\dot{\mathbf{u}} - \dot{\mathbf{U}}), \tag{2}$$

where $\underline{\boldsymbol{\sigma}}^s$ and $\underline{\boldsymbol{\sigma}}^f$ are the stress tensor of the solid and fluid phases, respectively. The homogenized densities related to the solid and fluid phases are ρ_{11} and ρ_{22}, while ρ_{12} relates to the interaction between the inertial forces of both phases. Finally, the viscous damping coefficient that accounts for the viscous iteration forces is $\tilde{b}$, while the gradient operator is ∇.

In a mathematical perspective, the aforementioned homogenized densities and damping coefficient can also be defined as [14],

$$\rho_{12} = -\phi\rho_f(\alpha_\infty - 1), \qquad \rho_{11} = (1-\phi)\rho_s - \rho_{12}, \qquad \rho_{22} = \phi\rho_f - \rho_{12}, \qquad \tilde{b} = \phi^2\sigma\tilde{G}(\omega), \tag{3}$$

with ϕ being the porosity, α_∞ the tortuosity, σ the static flow resistivity, ρ_f the fluid phase density and ρ_s the solid phase density. Following Johnson's model [15], $\tilde{G}(\omega)$ is written [16] as,

$$\tilde{G}(\omega) = \left[1 + \left(\frac{2\alpha_\infty\eta}{\phi\Lambda\sigma}\right)^2 \frac{j\omega\rho_f}{\eta}\right]^{1/2}. \tag{4}$$

Here, η is the fluid kinematic viscosity, Λ is the viscous characteristic length, ω is the angular frequency and $j^2 = -1$ is the imaginary number.

Assuming that the porous material properties are homogeneous and subject to harmonic oscillations, a more suitable way to describe the wave behavior in poroelastic materials was proposed by Atalla et al.

[14, 17], by turning Eqs. (1) and (2) into a mixed displacement-pressure ($\mathbf{u}/p$) formulation,

$$\nabla \cdot \hat{\underline{\boldsymbol{\sigma}}}^s + \omega^2 \tilde{\rho} \mathbf{u} + \tilde{\gamma} \nabla p = \mathbf{0}, \tag{5}$$

$$\nabla^2 p + \omega^2 \frac{\tilde{\rho_{22}}}{\tilde{R}} p - \omega^2 \frac{\tilde{\rho_{22}}}{\phi^2} \tilde{\gamma} \nabla \cdot \mathbf{u} = 0, \tag{6}$$

where the combined effective density $\tilde{\rho}$ and the coupling coefficient $\tilde{\gamma}$ are written as,

$$\tilde{\rho} = \tilde{\rho}_{11} - \frac{\tilde{\rho}_{12}^2}{\tilde{\rho}_{22}}, \quad \tilde{\gamma} = \phi \left(\frac{\tilde{\rho}_{12}}{\tilde{\rho}_{22}} - \frac{\tilde{Q}}{\tilde{R}} \right), \tag{7}$$

with the effective densities that account for the inertia effects in the solid ($\tilde{\rho}_{11}$), fluid ($\tilde{\rho}_{22}$) and in the viscous coupling that happens between the two ($\tilde{\rho}_{12}$) being,

$$\tilde{\rho}_{11} = \rho_{11} + \frac{\tilde{b}}{j\omega}, \qquad \tilde{\rho}_{22} = \rho_{22} + \frac{\tilde{b}}{j\omega}, \qquad \tilde{\rho}_{12} = \rho_{12} - \frac{\tilde{b}}{j\omega}. \tag{8}$$

The stress tensor of the porous material in vacuo $\hat{\underline{\boldsymbol{\sigma}}}^s$ also has a mathematical expression associated with it,

$$\hat{\underline{\boldsymbol{\sigma}}}^s = \left(\tilde{A} - \frac{\tilde{Q}^2}{\tilde{R}} \right) \nabla \cdot \mathbf{u} \mathbf{I} + 2N \underline{\boldsymbol{\varepsilon}}^s = \hat{A} \nabla \cdot \mathbf{u} \mathbf{I} + 2N \underline{\boldsymbol{\varepsilon}}^s, \tag{9}$$

where $\mathbf{I}$ is the identity tensor, $\tilde{A}$ is the first Lamé constant of the poroelastic material, N is the elastic shear modulus, $\tilde{Q}$ is the coupling coefficient between the dilatation of both component phases, $\tilde{R}$ is the bulk modulus of air occupying a fraction of volume aggregate and $\hat{A}$ is the first Lamé constant of the elastic phase [14, 18]. At last, since the majority of poroelastic media has high porosity in the applications here considered, the variables N, $\tilde{A}$, $\tilde{Q}$ and $\tilde{R}$ can be written in a simplified manner,

$$N = \frac{E(1 + j\eta_e)}{2(1+\nu)}, \qquad \tilde{A} = \frac{\nu E(1 + j\eta_e)}{(1+\nu)(1-2\nu)} \tag{10}$$

$$\tilde{Q} = (1-\phi)\tilde{K}_f, \qquad \tilde{R} = \phi \tilde{K}_f \tag{11}$$

where E, η_e and ν are the Young's modulus, the loss factor and the Poisson's ratio of the elastic material, respectively. $\tilde{K}_f$ is the bulk modulus of the air in the poroelastic material pores.

The weak form of Eqs. (5) and (6) is then obtained by the combination of the Weighted Residuals Method and the divergence theorem, followed by the consideration of material isotropy, that is [8, 19],

$$\int_{\Omega_p} \left\{ \hat{\underline{\boldsymbol{\sigma}}}^s(\mathbf{u}) : \underline{\boldsymbol{\varepsilon}}^s(\delta\mathbf{u}) - \omega^2 \tilde{\rho} \mathbf{u} \cdot \delta\mathbf{u} - (\tilde{\gamma} + \tilde{\xi}) \nabla p \cdot \delta\mathbf{u} - \tilde{\xi} p \nabla \cdot \delta\mathbf{u} \right\} d\Omega_p - \int_{\Gamma_p} (\underline{\boldsymbol{\sigma}}^t \cdot \mathbf{n}) \cdot \delta\mathbf{u} \, d\Gamma_p = \mathbf{0}, \tag{12}$$

$$\int_{\Omega_p} \left\{ \frac{\phi^2}{\omega^2 \tilde{\rho}_{22}} \nabla p \cdot \nabla \delta p - \frac{\phi^2}{\tilde{R}} p \delta p - (\tilde{\gamma} + \tilde{\xi}) \nabla \delta p \cdot \mathbf{u} - \tilde{\xi} \delta p \nabla \cdot \mathbf{u} \right\} d\Omega_p - \int_{\Gamma_p} \phi(\mathbf{U} - \mathbf{u}) \cdot \mathbf{n} \delta p \, d\Gamma_p = 0, \tag{13}$$

where $\delta\mathbf{u}$ and δp are test functions related to the solid phase displacement and the interstitial pressure, respectively, while Ω_p represents the poroelastic domain with Γ_p as its boundary. The newly introduced variable $\tilde{\xi} = \phi(1 + \tilde{Q}/\tilde{R})$ may be also viewed as a coupling coefficient, and $\mathbf{n}$ is the outward unit normal vector.

The Finite Element Method (FEM) [20] is then considered in the discretization of the aforementioned continuous problem, being also followed by Galerkin's approach. The result is a linear system of equations [16], as can be seen next,

$$\begin{bmatrix} \mathbf{K}-\omega^2\tilde{\mathbf{M}} & -(\tilde{\mathbf{C}}_1+\tilde{\mathbf{C}}_2) \\ -(\tilde{\mathbf{C}}_1+\tilde{\mathbf{C}}_2)^T & \tilde{\mathbf{H}}/\omega^2-\tilde{\mathbf{Q}} \end{bmatrix} \begin{Bmatrix} \mathbf{u} \\ \mathbf{p} \end{Bmatrix} = \begin{Bmatrix} \mathbf{f}_s \\ \mathbf{f}_p/\omega^2, \end{Bmatrix}, \tag{14}$$

where $\mathbf{K}$, $\tilde{\mathbf{M}}$, $\tilde{\mathbf{H}}$, $\tilde{\mathbf{Q}}$, $\tilde{\mathbf{C}}_1$, $\tilde{\mathbf{C}}_2$ denote the global stiffness, mass, kinetic, compression and coupling matrices, respectively. The global displacement and acoustic pressure vectors, as well as the global structural and acoustic loads are respectively defined as $\mathbf{u}$, $\mathbf{p}$, $\mathbf{f}_s$, $\mathbf{f}_p$.

3 UNIFIED MULTIPHASE MODELING: ACOUSTIC, ELASTIC AND POROELASTIC RELATIONS

In this technique, six variables are controlled, namely, $\tilde{\xi}$, $\tilde{\rho}$, N, $\hat{A}$, $\phi^2/\tilde{\rho}_{22}$ and $\phi^2/\tilde{R}$. For the acoustic case, these variables take the following values: 1, 0, 0, 0, $1/\rho_a$ and $1/\kappa_a$, where κ_a is the bulk modulus of the air (identified by the subscript a). For the elastic case, one gets the sequence: 0, ρ_e, N_e, $\tilde{A}_e$, 0 and 0, with the subscript e being related to the elastic material. In order to solve numerical issues that may appear with the above relations, small valued coefficients are assigned to each of the properties that have to be zero so that the final sequences get the following results,

$$\{\tilde{\xi},\tilde{\rho},N,\hat{A},(\phi^2/\tilde{\rho}_{22}),(\phi^2/\tilde{R})\}_p = \{\tilde{\xi},\tilde{\rho},N,\hat{A},\phi^2/\tilde{\rho}_{22},\phi^2/\tilde{R}\}, \tag{15}$$

$$\{\tilde{\xi},\tilde{\rho},N,\hat{A},(\phi^2/\tilde{\rho}_{22}),(\phi^2/\tilde{R})\}_a = \{1,\varepsilon_a\tilde{\rho},\varepsilon_a N,\varepsilon_a\hat{A},1/\rho_a,1/\kappa_a\}, \tag{16}$$

$$\{\tilde{\xi},\tilde{\rho},N,\hat{A},(\phi^2/\tilde{\rho}_{22}),(\phi^2/\tilde{R})\}_e = \{\varepsilon_e\tilde{\xi},\rho_e,N_e,\tilde{A}_e,\varepsilon_e(\phi^2/\tilde{\rho}_{22}),\varepsilon_e(\phi^2/\tilde{R})\}, \tag{17}$$

where the subscript p refers to the poroelastic material. Here, $\varepsilon_a = 1\times10^{-4}$ and $\varepsilon_e = 1\times10^{-9}$ were chosen.

The multiphase material interpolation scheme is then written,

$$\tilde{\xi} = \tilde{\xi}_e + x_2^{\zeta_2}(\tilde{\xi}_p-\tilde{\xi}_e) + x_1^{\zeta_1}(\tilde{\xi}_a-\tilde{\xi}_p), \tag{18}$$

$$\tilde{\rho} = \tilde{\rho}_e + x_2^{\zeta_2}(\tilde{\rho}_p-\tilde{\rho}_e) + x_1^{\zeta_1}(\tilde{\rho}_a-\tilde{\rho}_p), \tag{19}$$

$$N = N_e + x_2^{\zeta_2}(N_p-N_e) + x_1^{\zeta_1}(N_a-N_p), \tag{20}$$

$$\hat{A} = \hat{A}_e + x_2^{\zeta_2}(\hat{A}_p-\hat{A}_e) + x_1^{\zeta_1}(\hat{A}_a-\hat{A}_p), \tag{21}$$

$$\phi^2/\tilde{\rho}_{22} = (\phi^2/\tilde{\rho}_{22})_e + x_2^{\zeta_2}[(\phi^2/\tilde{\rho}_{22})_p-(\phi^2/\tilde{\rho}_{22})_e] + x_1^{\zeta_1}[(\phi^2/\tilde{\rho}_{22})_a-(\phi^2/\tilde{\rho}_{22})_p], \tag{22}$$

$$\phi^2/\tilde{R} = (\phi^2/\tilde{R})_e + x_2^{\zeta_2}[(\phi^2/\tilde{R})_p-(\phi^2/\tilde{R})_e] + x_1^{\zeta_1}[(\phi^2/\tilde{R})_a-(\phi^2/\tilde{R})_p], \tag{23}$$

where $x_{1,2}$ represents the design variables and the superscripts $\zeta_{1,2}$ are the penalty coefficients. After a series of tests, the following values were chosen for the design variables,

$$\{x_1,\ x_2\} = \{1,\ 1\}, \qquad \text{for acoustic elements,} \tag{24}$$

$$\{x_1,\ x_2\} = \{x_{\min},\ 1\}, \qquad \text{for poroelastic elements,} \tag{25}$$

$$\{x_1,\ x_2\} = \{x_{\min},\ x_{\min}\}, \qquad \text{for elastic elements,} \tag{26}$$

and for the penalty variables, $\{\zeta_1,\ \zeta_2\} = \{2,\ 2\}$. In order to avoid numerical singularities, $x_{\min} = 0.001$ is adopted, being the lower limit that the design variable can get. Table 1 shows the poroelastic and elastic material properties adopted in this work, while the acoustic characteristics used have been the same as the ones brought by Pereira et al. [9].

Table 1: Poroelastic and elastic material properties [6]

Parameters	Polyurethane foam	Olefin sheet
Porosity ϕ	0.97	–
Tortuosity α_∞	2.5	–
Static flow resistivity σ (N s m^{-4})	7×10^4	–
Viscous characteristic length Λ (μm)	36×10^{-6}	–
Thermal characteristic length Λ' (μm)	170×10^{-6}	–
Solid mass density ρ (kg m^{-3})	1433	1790
Young's modulus E (Pa)	2.67×10^5	1.75×10^8
Poisson ratio ν	0.4	0.4
Loss factor η	0.11	0.205

4 DESCRIPTION OF THE TOPOLOGY OPTIMIZATION PROBLEM

The topology optimization problem investigated in this work aims to maximize the time-averaged dissipated power (Π_{diss}) composed of its structural, viscous and thermal components. Throughout the numerical procedure, a frequency band of $[\omega_i,\ \omega_f]$ is also considered, together with the multimaterial and multiphysics constraints, therefore,

$$\text{Maximize: } \Phi = \frac{1}{\omega_f - \omega_i} \int_{\omega_i}^{\omega_f} 10 \log \frac{\Pi_{\text{diss}}}{\Pi_{\text{ref}}}\, \mathrm{d}\Omega_p, \quad \text{(in dB units)} \tag{27}$$

$$\text{Subjected to: } \begin{cases} \begin{bmatrix} \mathbf{K} - \omega^2 \tilde{\mathbf{M}} & -(\tilde{\mathbf{C}}_1 + \tilde{\mathbf{C}}_2) \\ -(\tilde{\mathbf{C}}_1 + \tilde{\mathbf{C}}_2)^T & \tilde{\mathbf{H}}/\omega^2 - \tilde{\mathbf{Q}} \end{bmatrix} \begin{Bmatrix} \mathbf{u} \\ \mathbf{p} \end{Bmatrix} = \begin{Bmatrix} \mathbf{f}_s \\ \mathbf{f}_p/\omega^2, \end{Bmatrix}, \\ \begin{Bmatrix} V_1^* - \left(\sum_{i=1}^{N_{\text{el}}} V_i x_i\right)_1 \\ V_2^* - \left(\sum_{i=1}^{N_{\text{el}}} V_i x_i\right)_2 \end{Bmatrix} = \begin{Bmatrix} 0 \\ 0 \end{Bmatrix}, \\ \underline{\mathbf{x}} = \left[\begin{Bmatrix} x_1 \\ \vdots \\ x_{N_{\text{el}}} \end{Bmatrix}_1, \begin{Bmatrix} x_1 \\ \vdots \\ x_{N_{\text{el}}} \end{Bmatrix}_2 \right]. \end{cases} \tag{28}$$

In Eq. (28), the prescribed final volume fraction is V^*, with the design domain volume fraction being $\sum_{i=1}^{N_{\text{el}}} V_i x_i$. N_{el} is the number of elements of the entire porous domain and $\underline{\mathbf{x}}$ is the design variable matrix. The subscript numbers 1 and 2 represent the changes along the optimization process, in other words, the number 1 refers to variations from acoustic to poroelastic elements, while the number 2 regards the changes from poroelastic to elastic.

Generally, the Π_{diss} formula can be obtained as,

$$\Pi_{\text{diss}} = \frac{\omega}{2} \begin{Bmatrix} \mathbf{u} \\ \mathbf{p} \end{Bmatrix}^H \text{Im} \left(\begin{bmatrix} \mathbf{K} - \omega^2 \tilde{\mathbf{M}} & -(\tilde{\mathbf{C}}_1 + \tilde{\mathbf{C}}_2) \\ -(\tilde{\mathbf{C}}_1 + \tilde{\mathbf{C}}_2)^T & \tilde{\mathbf{H}}/\omega^2 - \tilde{\mathbf{Q}} \end{bmatrix} \right) \begin{Bmatrix} \mathbf{u} \\ \mathbf{p} \end{Bmatrix}, \tag{29}$$

where the superscript H represents the transpose conjugate of the solution vector, Im() is the imaginary part and Π_{ref} is the reference acoustic power ($\Pi_{\text{ref}} = 1 \times 10^{-12}$ watts).

4.1 Sensitivity analysis

As the current work adopts the BESO method as the optimizer, the sensitivity analysis needs to be carried out to identify each elemental contribution to the maximization of the objective function of choice. The derivation of Eq. (27) follows,

$$\alpha_i = \frac{\mathrm{d}\Phi}{\mathrm{d}x_i} = \frac{1}{\omega_f - \omega_i} \left(\int_{\omega_i}^{\omega_f} \frac{10}{\ln 10} \frac{\mathrm{d}\Pi_{\text{diss}}/\mathrm{d}x_i}{\Pi_{\text{diss}}} \, \mathrm{d}\Omega_p \right), \tag{30}$$

with,

$$\frac{\mathrm{d}\Pi_{\text{diss}}}{\mathrm{d}x_i} = \frac{\partial \Pi_{\text{diss}}}{\partial x_i} + 2\text{Re} \left\{ \boldsymbol{\lambda}^T \left(\begin{bmatrix} \dfrac{\partial \mathbf{K}}{\partial x_i} - \omega^2 \dfrac{\partial \tilde{\mathbf{M}}}{\partial x_i} & -\left(\dfrac{\partial \tilde{\mathbf{C}}_1}{\partial x_i} + \dfrac{\partial \tilde{\mathbf{C}}_2}{\partial x_i} \right) \\ -\left(\dfrac{\partial \tilde{\mathbf{C}}_1}{\partial x_i} + \dfrac{\partial \tilde{\mathbf{C}}_2}{\partial x_i} \right)^T & \dfrac{1}{\omega^2} \dfrac{\partial \tilde{\mathbf{H}}}{\partial x_i} - \dfrac{\partial \tilde{\mathbf{Q}}}{\partial x_i} \end{bmatrix} \begin{Bmatrix} \mathbf{u} \\ \mathbf{p} \end{Bmatrix} - \begin{Bmatrix} \dfrac{\partial \mathbf{f}_s}{\partial x_i} \\ \dfrac{1}{\omega^2} \dfrac{\partial \mathbf{f}_p}{\partial x_i} \end{Bmatrix} \right) \right\} \tag{31}$$

and,

$$\begin{bmatrix} \mathbf{K} - \omega^2 \tilde{\mathbf{M}} & -(\tilde{\mathbf{C}}_1 + \tilde{\mathbf{C}}_2) \\ -(\tilde{\mathbf{C}}_1 + \tilde{\mathbf{C}}_2)^T & \tilde{\mathbf{H}}/\omega^2 - \tilde{\mathbf{Q}} \end{bmatrix} \boldsymbol{\lambda} = -\frac{1}{2} \left(\frac{\partial \Pi_{\text{diss}}}{\partial \left(\text{Re} \begin{Bmatrix} \mathbf{u} \\ \mathbf{p} \end{Bmatrix} \right)} - j \frac{\partial \Pi_{\text{diss}}}{\partial \left(\text{Im} \begin{Bmatrix} \mathbf{u} \\ \mathbf{p} \end{Bmatrix} \right)} \right)^T, \tag{32}$$

where Re() represents the real part.

5 NUMERICAL EXAMPLES

This section presents numerical examples regarding the optimization of the system illustrated in Fig. 1. Here, the design, Ω_d, and the non-design, Ω_{nd}, domains are represented by the grey region at the center of the system, and by the white and black areas located at the sides, respectively. Initially, poroelastic structures fill the entire Ω_d, while acoustic and elastic elements are set in the major white areas and on the thin walls surrounding the design domain. At the upper and lower sides, symmetric boundary conditions are imposed (only the degrees of freedom in the y direction are blocked); a plane wave enters the composition at the left boundary, while at the right, an anechoic termination is set.

In the represented scenario, first order quadrilateral elements of size 1x1,25 mm^2 are considered, meaning that 22x40 elements are placed at both sides of Ω_{nd} and 80x40 in Ω_d. The BESO parameters are then set to be $\text{ER} = \text{AR}_{\text{max}} = 1\%$ and $r_{\text{min}} = 2$ cm. Besides, $V_2^* = 0.05$ is fixed, defining the amount of elastic material that enters the design domain along the optimization procedure. Meanwhile, V_1^* is variable, that is, in some cases $V_1^* = 0.5$ and in others $V_1^* = 0.6$. Besides, two distinct low-to-mid multifrequency bands are also treated in this work, namely B1 = [150, 200] Hz and B2 = [200, 250].

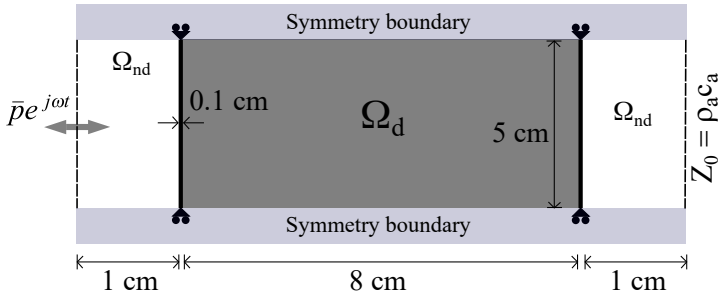

Figure 1: Schematic representation of the considered geometry

Fig. 2 shows the optimized results obtained from the maximization of the time-averaged dissipated powers when considering multiple frequency bands and distinct porous volume fractions. In Fig. 2 (a) and (c), the topologies are strongly related to one another, with the one of item (c) being the most effective in enhancing the objective function (see Fig. 2 (e)). This same aspect is not observed in Fig. 2 (b) and (d), where B2 is considered. In this case, the topologies are entirely different, with the case of 50% of porous material being similar, from a purely dissipative point of view, to its counterpart. This unsuspected result illustrates how efficient the proposed topology optimization methodology can be, as effective topologies may be generated with less material than expected. Finally, it is noted that even though some topologies may present disconnected porous materials, such characteristic does not affect, in a considerable manner, the dissipative effects of the main resulted topologies.

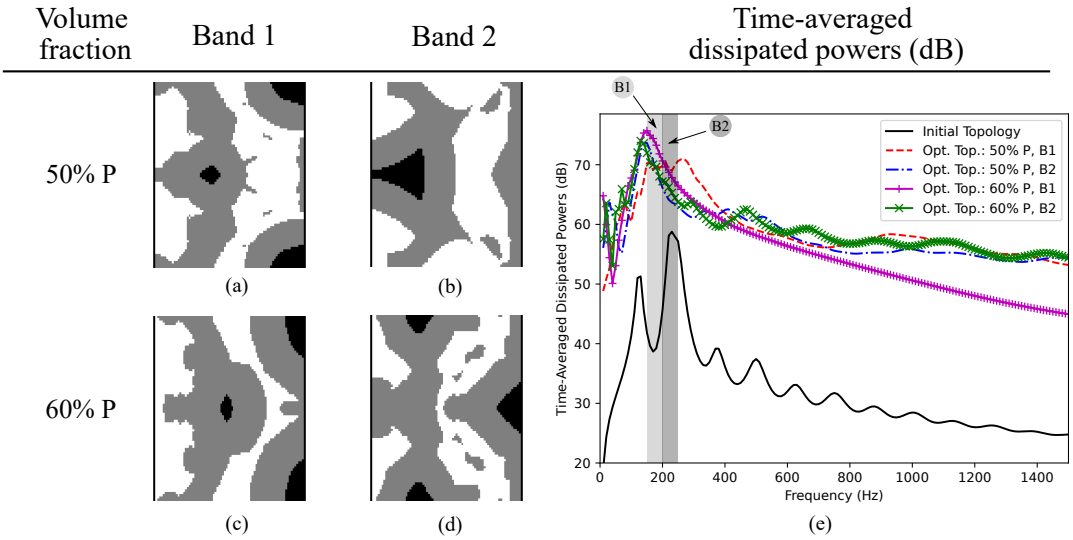

Figure 2: Optimized topologies when considering (a) 50% and (c) 60% of porous material in band 1, together with (b) 50% and (d) 60% in band 2. (e) The initial and final time averaged-dissipated powers are also shown

6 CONCLUSIONS

This work proposed a multifrequency topology optimization methodology to maximize time-averaged dissipated powers of an acoustic-poroelastic-elastic structure. For this, the Bi-directional Evolutionary Structural Optimization approach was considered as the optimizer, in order to provide clearly defined designs throughout the iterative procedure. The unified multiphase technique was then combined with the finite element method to fully describe elastic and acoustic systems, starting from Biot's poroelasticity equations. This combination proved to be an efficient solution to the boundary tracking problem, common to fluid-structure systems.

Furthermore, a newly introduced material interpolation scheme was also proposed, systematically combining acoustic-poroelastic-elastic properties. With this, the numerical examples showed to be highly effective in maximizing the objective function while generating topologies with low material disconnections.

REFERENCES

[1] Xie, Y. and Steven, G. P. A simple evolutionary procedure for structural optimization. *Comput. Struct.* (1993) **49**:885–896.

[2] Yang, X. Y., Xie, Y. M., Steven, G. P. and Querin, O. M. Bidirectional evolutionary method for stiffness optimization. *AIAA J.* (1999) **37**:1483–1488.

[3] Sigmund, O. and Petersson, J. Numerical instabilities in topology optimization: A survey on procedures dealing with checkerboards, mesh-dependencies and local minima. *Struct. Optim* (1998) **16**:68–75.

[4] Bendsøe, M. P. and Sigmund, O. Material interpolation schemes in topology optimization. *Arch. Appl. Mech.* (1999) **69**:635–654.

[5] Huang, X. and Xie, Y. M. *Evolutionary Topology Optimization of Continuum Structures: Methods and Applications*. Ed. John Wiley & Sons, Vol. I., (2010).

[6] Yamamoto, T., Maruyama, S., Nishiwaki, S. and Yoshimura, M. Topology design of multi-material soundproof structures including poroelastic media to minimize sound pressure levels. *Comput. Method Appl. M.* (2009) **198**:1439–1455.

[7] Lee, J. S. *Unified Multi-Phase Modeling and Topology Optimization for Complex Vibro-Acoustic Systems Consisting of Acoustic, Poroelastic and Elastic Media*. School of Mechanical and Aerospace Engineering, The Graduate School, Seoul National University, (2009).

[8] Lee, J. S., Kang, Y. J. and Kim, Y. Y. Unified multiphase modeling for evolving, acoustically coupled systems consisting of acoustic, elastic, poroelastic media and septa. *J. Sound Vib.* (2012) **331**:5518–5536.

[9] Pereira, R. L., Lopes, H. N. and Pavanello, R. Topology optimization of acoustic systems with a multiconstrained BESO approach. *Finite Elem. Anal. Des.* (2022) **201**:103701.

[10] Picelli, R., Vicente, W., Pavanello, R. and Xie Y. Evolutionary topology optimization for natural frequency maximization problems considering acoustic–structure interaction. *Finite Elem. Anal. Des.* (2015) **106**:56–64.

[11] Vicente, W., Picelli, R., Pavanello, R. and Xie Y. Topology optimization of frequency responses of fluid–structure interaction systems. *Finite Elem. Anal. Des.* (2015) **98**:1–13.

[12] Biot, M. A. Theory of Propagation of Elastic Waves in a Fluid-Saturated Porous Solid: I. Low-Frequency Range. *J. Acoust. Soc. Am.* (1956) **28**:168–178.

[13] Biot, M. A. Theory of Propagation of Elastic Waves in a Fluid-Saturated Porous Solid: II. Higher-Frequency Range. *J. Acoust. Soc. Am.* (1956) **28**:179–191.

[14] Atalla, N., Panneton, R. and Debergue, P. A mixed displacement-pressure formulation for poroelastic materials. *J. Acoust. Soc. Am.* (1998) **104**:1444–1452.

[15] Johnson, D. L., Koplik, J. and Dashen, R. Theory of dynamic permeability and tortuosity in fluid-saturated porous media. *J. Fluid Mech.* (1987) **176**:379–402.

[16] Allard, J. F. and Atalla, N. *Propagation of Sound in Porous Media: Modelling Sound Absorbing Materials*. Ed. John Wiley & Sons, Vol. I. (1993), Vol. II. (2009).

[17] Atalla, N., Hamdi, M. A. and Panneton, R. Enhanced weak integral formulation for the mixed (u,p) poroelastic equations. *J. Acoust. Soc. Am.* (2001) **109**:3065–3068.

[18] Lee, J. S., Göransson, P. and Kim, Y. Y. Topology optimization for three-phase materials distribution in a dissipative expansion chamber by unified multiphase modeling approach. *Comput. Method Appl. M.* (2015) **287**:191–211.

[19] Rigobert, S., Atalla, N. and Sgard, F. C. Investigation of the convergence of the mixed displacement-pressure formulation for three-dimensional poroelastic materials using hierarchical elements. *J. Acoust. Soc. Am.* (2003) **114**:2607–2617.

[20] Atalla, N. and Sgard, F. *Finite Element and Boundary Methods in Structural Acoustics and Vibration*. Ed. CRC Press, Vol. I., (2015).